

# Modeling of subgrid effects in coarse-scale simulations of transport in heterogeneous porous media

Y. Efendiev

Institute for Mathematics and Its Applications, University of Minnesota, Minneapolis

L. J. Durlofsky<sup>1</sup>

Department of Petroleum Engineering, Stanford University, Stanford, California

S. H. Lee

Chevron Petroleum Technology Company, San Ramon, California

**Abstract.** A methodology for incorporating subgrid effects in coarse-scale numerical models of flow in heterogeneous porous media is presented. The method proceeds by upscaling the deterministic fine-grid permeability description and then solving the pressure equation over the coarse grid to obtain coarse-scale velocities. The coarse-grid saturation equation is formed through a volume average of the fine-scale equations and includes terms involving both the average and fluctuating components of the velocity field. The terms involving the fluctuating components are subgrid effects that appear as length- and time-dependent dispersivities. A simplified model for the coarse-scale dispersivity, in terms of these subgrid velocity fluctuations, is proposed, and a numerical scheme based on this model is implemented. Results using the new method are presented for a variety of two-dimensional heterogeneous systems characterized by moderate permeability correlation length in the dominant (horizontal) flow direction and small correlation length in the vertical direction. The new method is shown to provide much more accurate results than comparable coarse-grid models that do not contain the subgrid treatment. Extensions of the overall methodology to handle more general systems are discussed.

## 1. Introduction

Subsurface formations typically exhibit heterogeneities over a wide range of length scales. Because only a limited amount of data are generally available, formation properties are often described using some type of geostatistical approach. Flow and transport results for such descriptions reflect the uncertainty associated with the geological model. Within this general stochastic framework, two different approaches are commonly used. The first approach entails a stochastic formulation of the flow equations. The second approach is a Monte Carlo methodology that requires the simulation of multiple realizations of the heterogeneous formation.

Using the first approach, formation properties are represented in the flow equations as random variables. The resulting flow quantities are then also random variables, that is, described in terms of expected values and higher statistical moments [Dagan, 1987; Gelhar, 1993]. This formulation is highly desirable because, from a single solution of the flow problem, a statistical description of the relevant flow parameters can be determined. However, this approach also has some limitations. Specifically, the set of equations that must be solved is, in general, considerably more complex than the underlying deterministic equations [Graham and McLaughlin, 1989; Neu-

man, 1993]. Further, it is often difficult to include additional physics (e.g., three-phase flow) or other complications, such as different geostatistical models in different regions of the formation, without extensive reformulation.

Using the second, Monte Carlo approach, multiple realizations of the heterogeneous formation are generated, and each is then simulated deterministically [Hewett and Behrens, 1990]. In this approach, there is no uncertainty associated with the formation properties or the flow results for any single realization (other than errors due to numerical discretization). The probability distribution associated with the flow problem is determined through the simulation of multiple realizations of the formation. The complication in this case is that each realization must be highly detailed in order to capture all of the relevant scales of heterogeneity. This renders the simulation of even a single realization demanding. The handling of multiple realizations represents an even greater challenge.

Upscaling procedures are commonly used to coarsen these highly detailed geostatistical realizations to scales more suitable for flow simulation. A variety of such approaches exists, and there are advantages and disadvantages associated with the different methodologies (for recent reviews, see Christie [1996] and Wen and Gomez-Hernandez [1996]). In general, there is somewhat of a trade-off between robustness and computational efficiency. Robustness in this context refers to process independence, meaning the same coarse-scale description is applicable for different flow processes; for example, different boundary and initial conditions. Less robust approaches typically achieve higher degrees of coarsening, but their use for problems which significantly deviate from the base case (used

<sup>1</sup>Also at Chevron Petroleum Technology Company, San Ramon, California.

to compute the coarse-scale model parameters) can be suspect (see *Durlofsky* [1997, 1998] and *Barker and Thibeau* [1997] for further discussion).

The purpose of this paper is to present the numerical implementation of a moment-based methodology for the upscaling of detailed geostatistical models. This procedure is directly applicable to the Monte Carlo modeling approach and serves to greatly reduce the computation time required for flow modeling for each geostatistical realization. Our upscaling approach is intended to generate robust, highly coarsened models appropriate for the description of transport processes in heterogeneous formations with moderate to large correlation length in the dominant flow direction. Such correlation structures are commonly encountered in oil reservoirs and aquifers.

Our methodology is distinct from previous work in which the flow equations are formulated stochastically, because the averages we consider are volume averages (rather than ensemble averages) and the moments are correspondingly spatial (rather than statistical). However, the governing equations are similar to those obtained within the stochastic framework. The solution procedures are quite different, however, because we cannot rely on ensemble-averaged quantities to provide the coarse-scale coefficients appearing in our transport equations.

The approach described in this paper also differs considerably from previous methods for upscaling. Most such methods either attempt to minimize, and then neglect, subgrid effects [*Durlofsky et al.*, 1996, 1997] or require the a priori estimate of the global flow field from which upscaled (or pseudo) flux functions are computed [*Christie*, 1996; *Barker and Thibeau*, 1997]. The present method does model subgrid effects, but it does not require a priori estimates of the global flow field. This is possible because the coarse-grid block parameters evolve in time as the calculation proceeds.

Our approach shares some elements with the large eddy simulation (LES) methodology described by *Beckie et al.* [1994, 1996]. However, in our upscaling of the underlying pressure equation we apply a nonuniform coarsening procedure [*Durlofsky et al.*, 1996, 1997]. This method introduces variable degrees of coarsening throughout the domain, with more refinement in active regions (typically connected regions of high permeability leading to high flow rates and early breakthrough) and more coarsening in less active regions. This approach, which defines our averaging volumes, does not correspond to any specific filter applied in the LES approach. In addition, our volume averages are defined discretely (over regions corresponding to coarse-scale grid blocks) rather than continuously. As a result, our coarse-scale equations differ somewhat from those of *Beckie et al.* [1994, 1996]. Nonetheless, the basic idea of representing subgrid effects in terms of scale-dependent coarse-grid models is shared by the two methods.

In recent work, *Rubin et al.* [1999] applied a related approach within a stochastic framework to compute block-effective macrodispersivities. They considered the case where fine-scale details of the permeability field are represented statistically and the permeability field is of correlation length that is small relative to the system size. They treat systems for which the velocity covariance function is stationary and can be computed from the covariance of log permeability. For this case they computed coarse-scale dispersivities as a function of time and block size (relative to the permeability correlation length). Though they did not present any global coarse-scale flow results, their block-effective macrodispersivities could be applied

in large-scale flow simulations for the types of systems they considered.

Our work here in some respects complements the earlier work of *Rubin et al.* [1999]. We address two-phase flow (*Rubin et al.* restricted themselves to single-phase flow) though we present results for only the single-phase case. In addition, we consider specific realizations of the permeability field (in which permeability is specified in every fine-grid block). We are also interested in the case of larger permeability correlation lengths, with the correlation length typically exceeding the size of the coarse-scale blocks in the  $x$  direction. As a result, our velocity fields are nonstationary, and the velocity covariance cannot be computed a priori. Rather, we estimate the magnitude of subgrid velocity variations from limited fine-scale calculations. Our results are, however, preasymptotic (valid at early time), while *Rubin et al.* compute macrodispersivities for all times (including the long-time asymptote). Though the two studies apply different approaches and emphasize different parameter ranges, the preasymptotic results of *Rubin et al.* may correspond to the dispersivities we compute in this paper in some cases. A detailed comparison of the two approaches will require further investigation.

This paper proceeds as follows. In section 2 we present the equations governing flow at the fine scale and briefly discuss previous upscaling approaches. We present the averaged saturation and moment equations and simplify these equations for the unit mobility ratio case in section 3. Next, in section 4, we describe our numerical procedure for the solution of the coarse-grid equations. Coarse-scale flow results for a variety of heterogeneous two-dimensional systems are presented in section 5. Further discussion and conclusions are presented in section 6.

## 2. Governing Equations and Upscaling Procedures

Our interest is in developing a methodology applicable for the coarse-scale modeling of two-phase flow in heterogeneous systems. We will present the governing equations for this case but will then apply our method to a simpler, unit mobility ratio displacement. This case is identical to the purely advective contaminant transport model. In subsequent work we will present the application of the overall approach to the two-phase flow case. Some aspects of the two-phase flow problem are treated by *Efendiev* [1999].

Because we are most interested in modeling the effects of permeability heterogeneity on the flow, we will simplify the problem by neglecting the effects of gravity, compressibility, and capillary pressure. Porosity will be considered to be constant. We refer to the two phases as water and oil. Darcy's law for each phase, with all quantities dimensionless, can then be written as follows:

$$\mathbf{v}_j = -\frac{k_{rj}(S)}{\mu_j} \mathbf{k} \cdot \nabla p. \quad (1)$$

Here  $\mathbf{v}_j$  represents the Darcy's velocity for the phase  $j$  ( $j = o$  (oil), and  $j = w$  (water)),  $k_{rj}$  is the phase relative permeability,  $\mu_j$  is the phase viscosity,  $p$  is the pressure (which is the same for both phases because capillary pressure effects are neglected), and  $S$  is the saturation (volume fraction) of water. The permeability tensor  $\mathbf{k}$ , taken to be diagonal, shows a high degree of spatial variation. A single set of relative permeability curves will be assumed to apply throughout the domain.

These constitutive equations, coupled with a statement of mass conservation ( $\nabla \cdot (\mathbf{v}_o + \mathbf{v}_w) = 0$ ), can be expressed in terms of the so-called pressure and saturation equations:

$$\nabla \cdot (\lambda(S)\mathbf{k} \cdot \nabla p) = 0, \quad (2a)$$

$$\frac{\partial S}{\partial t} + \mathbf{v} \cdot \nabla f(S) = 0. \quad (2b)$$

The parameters in (2) are given as

$$\lambda(S) = \frac{k_{rw}(S)}{\mu_w} + \frac{k_{ro}(S)}{\mu_o}, \quad (3a)$$

$$f(S) = \frac{k_{rw}(S)/\mu_w}{k_{rw}(S)/\mu_w + k_{ro}(S)/\mu_o}, \quad (3b)$$

$$\mathbf{v} = \mathbf{v}_w + \mathbf{v}_o = -\lambda(S)\mathbf{k} \cdot \nabla p. \quad (3c)$$

Here  $\lambda(S)$  is referred to as the total mobility, and  $f(S)$  is the fractional flow function. For the unit mobility ratio case considered below,  $\lambda(S) = 1$  and  $f(S) = S$ .

Our intent here is to develop a coarse-scale description for two-phase flow in heterogeneous porous media. Previous approaches for upscaling include the use of pseudo relative permeabilities and/or the use of nonuniform coarsening. Pseudo relative permeability approaches entail the use of upscaled (pseudo) relative permeabilities ( $k_{rj}^*$ ) in place of the  $k_{rj}$  in (2) and (3). These functions are typically generated through the solution of local fine-scale flow problems, subject to assumed boundary conditions for pressure and saturation, and the subsequent calculation of coarse-grid parameters. These coarse-grid parameters are computed such that they provide the same average response as the fine-grid model for the prescribed boundary conditions.

This approach can achieve high degrees of coarsening, though the coarse-scale parameters can exhibit a high degree of dependence on the (assumed) boundary conditions for the local flow problem in some cases. This, in turn, can lead to a lack of robustness in the coarse-scale description. See *Christie* [1996] and *Barker and Thibeau* [1997] for further discussion of the overall approach. Recent work has demonstrated that the calculation of pseudo relative permeabilities using local boundary conditions based on effective medium theory can lead to significantly improved coarse-scale results [*Wallstrom et al.*, 2000]. However, the robustness of the overall approach is still being assessed.

Nonuniform coarsening approaches, with no upscaling of relative permeabilities, represent an alternative to the use of pseudo relative permeabilities. These methods act to generate coarsened models with more resolution in high-flow regions and less resolution in slower regions [*Durlofsky et al.*, 1996, 1997]. The coarse model is therefore capable of capturing effects due to the high extremes of the permeability field, such as the early breakthrough of injected fluids. Nonuniform coarsening approaches, however, can typically attain only moderate degrees of coarsening (e.g., a factor of 3–5 in each coordinate direction). To achieve higher degrees of coarsening, some type of subgrid model will be required.

Our ultimate goal is to develop a robust, highly coarsened (e.g., coarsened by a factor of  $\sim 10$  in each coordinate direction) description of the subsurface. This will require the use of coarse-scale parameters that are not strongly dependent on a priori assumptions about the global fine-scale flow field. Ideally, such a model would use only local fine-scale flow solutions

coupled with global coarse-scale information. Such a capability would avoid the need to solve global fine-scale flow problems, while at the same time providing accurate estimates of subgrid effects for a wide variety of global boundary specifications.

In previous studies it has been demonstrated that the coarse-scale pressure equation can be taken to be of the same form as the fine-scale equation but with an equivalent grid block permeability tensor  $\mathbf{k}^*$  in place of  $\mathbf{k}$ . See *Durlofsky* [1991] and *Renard and de Marsily* [1997] for detailed discussions on the calculation of  $\mathbf{k}^*$ . Numerical solutions of the coarse-scale pressure equation formed in this way have been shown to provide integrated flow quantities in close agreement with the corresponding fine-scale results. More difficulties are typically encountered in upscaling the saturation equation. Owing to the hyperbolic nature of this equation and the high correlation length features often present in the fine-scale permeability field, distant (nonlocal) effects can strongly impact coarse-grid parameters. It is for this reason that coarse-grid properties are often dependent on global boundary conditions. Therefore our focus here will be on obtaining a robust subgrid model for use in the saturation equation.

As we will see, the model developed here is not completely general, though it does have several desirable characteristics. These include an explicit dependence on local subgrid information and an explicit coupling between the local fine-scale response and the global flow field. As discussed in section 3, local fine-scale flow information may be available from the solutions of the local fine-scale pressure equation, used in the calculation of  $\mathbf{k}^*$ , or via the use of multiscale finite element methods [*Hou and Wu*, 1997; *Efendiev*, 1999].

### 3. Volume-Averaged Description

Our approach here entails a volume average (area average in two dimensions) of the fine-grid saturation equation ((2b) above) over regions corresponding to coarse grid blocks. The details of the volume-averaging procedure were presented previously [*Durlofsky*, 1998]. Volume-averaged equations are generated by expressing fine-scale quantities as the sum of volume-averaged and fluctuating components; that is

$$\Phi(x, z) = \bar{\Phi} + \Phi'(x, z), \quad (4a)$$

where  $\Phi$  is any fine-grid quantity. The overbar indicates a volume-averaged quantity (constant throughout the averaging region), and the prime denotes a spatially varying fluctuating quantity. The volume average is defined as

$$\bar{\Phi} = \frac{1}{A} \int_D \Phi(x, z) dx dz, \quad (4b)$$

where  $D$  denotes the region within the coarse-grid block and  $A$  is the area; that is, we average fine-grid quantities over regions corresponding to the coarse-grid blocks. Using this notation,  $\bar{S}$ ,  $\bar{\mathbf{v}}$ , and  $\bar{f}$  are now coarse-scale functions (constants in each coarse block), while  $S'$ ,  $\mathbf{v}'$ , and  $f'$  are fluctuating functions in each coarse block. Inserting these representations for  $S$ ,  $f$ , and  $\mathbf{v}$  into (2b) and then averaging the resulting equation gives the averaged saturation equation:

$$\frac{\partial \bar{S}}{\partial t} + \bar{\mathbf{v}} \cdot \nabla \bar{f} + \overline{\mathbf{v}' \cdot \nabla f'} = 0. \quad (5)$$

The fluctuating equation is then obtained by subtracting (5) from the fine-scale equation. This gives the equation for  $S'$  as follows:

$$\frac{\partial S'}{\partial t} + \bar{\mathbf{v}} \cdot \nabla f' + \mathbf{v}' \cdot \nabla \bar{f} + \mathbf{v}' \cdot \nabla f' = \overline{\mathbf{v}' \cdot \nabla f'}. \quad (6)$$

In (5) and (6),  $\bar{S}$ ,  $\bar{\mathbf{v}}$ , and  $\bar{f}$  are semidiscrete quantities; that is, they are constant in each grid block and are discontinuous across block boundaries. These equations are written based on the recognition that they will be solved using a numerical, finite volume scheme. In this case, as we shall see below, quantities such as  $\nabla \bar{f}$  (or  $\nabla \bar{S}$ ) are evaluated at block boundaries and involve differences of  $\bar{S}$  across block edges. Thus the coarse-scale equations are not strictly continuous and are best understood with reference to a particular type of numerical method.

Equations quite similar to (5) and (6) can be derived using a spatial filtering approach [Beckie *et al.*, 1994, 1996], in which case the coarse-scale variables are continuous rather than discrete. In this case, additional terms appear in the coarse-scale equations. In the averaged (filtered) coarse-scale saturation equation, for example (this equation is analogous to (5)), extra terms of the form  $\bar{\mathbf{v}} \cdot \nabla f'$  and  $\mathbf{v}' \cdot \nabla \bar{f}$  appear. These terms, referred to as “cross terms” by Beckie *et al.* [1994, 1996], are identically zero in our formulation because  $\bar{\mathbf{v}}$  and  $\bar{f}$  are constant over the control volumes and  $\bar{\mathbf{v}}$  and  $\bar{f}$  are zero. In the filtered equations, however, the cross terms are nonzero because averaged (or filtered) quantities vary continuously.

Though these extra terms appear in the filtered equations, the differences between the discrete solution of the filtered equations and the discrete solution of (5) above are only  $O(h)$ , where  $h$  is the size of a grid block in the numerical solution. The differences between these two formulations are relatively small because averaged quantities are assumed to have some degree of smoothness on the coarse scale. If this is not the case, then there could be more significant differences between the two formulations. It is, however, important to recognize that our model for subgrid effects, introduced below, is approximate. We expect that the differences between our averaged equation and the filtered equations of Beckie *et al.* [1994, 1996] are small compared to the approximations introduced in the subgrid model.

Using (5) and (6), we now develop a coarse model for the unit mobility case; that is,  $f(S) = S$ . This type of model has been derived and used previously in the stochastic framework [Dagan, 1984; Kitanidis, 1988; Rubin, 1990; Zhang, 1995; Rubin *et al.*, 1999], so the form of the resulting equations is familiar. Langlo and Espedal [1994] and Zhang *et al.* [1999] further developed numerical models, again within the stochastic framework, for the two-phase case.

In the derivation of the coarse model we assume that the fluctuations in the saturation and velocity fields are small; that is, we neglect terms involving products of three fluctuating quantities. This clearly introduces some approximation into our method. However, because we generate the coarse-grid structure using the nonuniform coarsening methodology, the subgrid variation of the velocity in each coarse block will be reduced to some extent.

The equations for the averaged and fluctuating components of the saturation in the unit mobility ratio case are

$$\frac{\partial \bar{S}}{\partial t} + \bar{\mathbf{v}} \cdot \nabla \bar{S} + \overline{\mathbf{v}' \cdot \nabla S'} = 0, \quad (7)$$

$$\frac{\partial S'}{\partial t} + \bar{\mathbf{v}} \cdot \nabla S' + \mathbf{v}' \cdot \nabla \bar{S} + \mathbf{v}' \cdot \nabla S' = \overline{\mathbf{v}' \cdot \nabla S'}. \quad (8)$$

For our finite volume numerical solution it will be useful to rewrite the averaged (7) as

$$\frac{\partial \bar{S}}{\partial t} + \frac{1}{A} \int_{\partial D} (\bar{\mathbf{v}} \cdot \mathbf{n}) \bar{S} \, dl + \frac{1}{A} \int_{\partial D} (\mathbf{v}' \cdot \mathbf{n}) S' \, dl = 0, \quad (9)$$

where averaged quantities are now interpreted as averages over coarse-block edges and fluctuating quantities are computed analogously. The average velocity over the coarse block can now be defined as the average of the velocities at the four edges. It is evident from (9) that, in our numerical solution,  $\nabla \bar{S}$  at cell edges is represented in terms of differences of  $\bar{S}$  in neighboring cells. Within a cell,  $\bar{S}$  is represented in the numerical method as piecewise linear; that is, we compute second-order accurate fluxes using slope-limited representations of  $\bar{S}$  at the cell edges.

To proceed further, we need to estimate the  $\overline{\mathbf{v}' \cdot \nabla S'}$  term in (7). We accomplish this through use of (8). Specifically, we project (8) onto the coarse-grid streamlines, defined via  $d\mathbf{x}/dt = \bar{\mathbf{v}}$ . The  $\partial S'/\partial t$  and  $\bar{\mathbf{v}} \cdot \nabla S'$  terms can then be combined, giving the fluctuating equation expressed along trajectories corresponding to streamlines (in this and subsequent equations we apply summation notation, where summation over repeated subscripts is implied):

$$\frac{dS'(t, \mathbf{x}(t))}{dt} + v'_j \nabla_j \bar{S} + v'_j \nabla_j S' = \overline{v'_j \nabla_j S'}. \quad (10)$$

For each  $(\mathbf{x}, t)$ , such that  $\mathbf{x}(t) = \mathbf{x}$ , integrating (10) over  $(0, t)$  we have

$$\begin{aligned} S'(t, \mathbf{x}) = & - \int_0^t [v'_j(\mathbf{x}(\tau)) \nabla_j \bar{S}(\tau, \mathbf{x}(\tau)) \\ & + v'_j(\mathbf{x}(\tau)) \nabla_j S'(\tau, \mathbf{x}(\tau))] \, d\tau \\ & + \int_0^t \overline{v'_j(\mathbf{x}(\tau)) \nabla_j S'(\tau, \mathbf{x}(\tau))} \, d\tau. \end{aligned} \quad (11)$$

Multiplying (11) by  $v'_i(\mathbf{x})$  and averaging over the boundaries of a coarse block  $D$ , we obtain

$$\begin{aligned} \int_{\partial D} S'(t, \mathbf{x}) v'_i(\mathbf{x}) n_i \, dl = & \\ & - \int_{\partial D} \int_0^t v'_i(\mathbf{x}) v'_j(\mathbf{x}(\tau)) n_i \nabla_j \bar{S}(\tau, \mathbf{x}(\tau)) \, d\tau \, dl \\ & - \int_{\partial D} \int_0^t v'_i(\mathbf{x}) v'_j(\mathbf{x}(\tau)) n_i \nabla_j S'(\tau, \mathbf{x}(\tau)) \, d\tau \, dl \\ & + \int_{\partial D} \int_0^t \overline{v'_i(\mathbf{x}) v'_j(\mathbf{x}(\tau)) \nabla_j S'(\tau, \mathbf{x}(\tau))} \, d\tau \, dl. \end{aligned} \quad (12)$$

The last term in (12) is equal to zero because  $\bar{\mathbf{v}}' = 0$  for each edge. We further neglect the term containing  $\mathbf{v}' \mathbf{v}' S'$  because it is third order in fluctuating quantities. We are then left with

$$\int_{\partial D} S'(t, \mathbf{x}) v'_i n_i dl \approx - \int_{\partial D} \int_0^t v'_i(\mathbf{x}) v'_j(\mathbf{x}(\tau)) n_i \nabla_j \bar{S}(\tau, \mathbf{x}(\tau)) d\tau dl. \quad (13)$$

Substituting this expression into (9),

$$\frac{\partial \bar{S}}{\partial t} + \frac{1}{A} \int_{\partial D} \bar{v}_j n_j \bar{S} dl = \frac{1}{A} \int_{\partial D} \int_0^t v'_i(\mathbf{x}) v'_j(\mathbf{x}(\tau)) n_i \nabla_j \bar{S}(\tau, \mathbf{x}(\tau)) d\tau dl. \quad (14)$$

Equation (14) can be simplified by noting that the time derivative of  $\bar{S}$  along streamlines is small. Equation (14) can now be expressed as

$$\frac{\partial \bar{S}}{\partial t} + \frac{1}{A} \int_{\partial D} \bar{v}_j n_j \bar{S} dl = \frac{1}{A} \int_{\partial D} \left[ \int_0^t v'_i(\mathbf{x}) v'_j(\mathbf{x}(\tau)) d\tau \right] n_i \nabla_j \bar{S}(t, \mathbf{x}) dl. \quad (15)$$

At a given time in our finite volume solution procedure,  $\nabla_j \bar{S}(t, \mathbf{x})$  is a quantity determined by the difference of neighboring values of  $\bar{S}$  in the coarse blocks with the common edge  $\partial E$ . Then the dispersive flux across the edge  $\partial E$  in (15), referred to as  $j_E$ , becomes

$$j_E = \frac{1}{A} \int_{\partial E} \left[ \int_0^t v'_i(\mathbf{x}) v'_j(\mathbf{x}(\tau)) d\tau \right] n_i dl \nabla_j \bar{S}(t, \mathbf{x}). \quad (16a)$$

The total dispersive flux  $j_t$  into the coarse block  $D$  is defined as the sum of the dispersive fluxes across the four edges of the coarse block:

$$j_t = \frac{1}{A} \sum_{p=1}^4 \left\{ \int_{\partial E_p} \left[ \int_0^t v'_i(\mathbf{x}) v'_j(\mathbf{x}(\tau)) d\tau \right] n_i dl \nabla_j \bar{S}(t, \mathbf{x}) \right\}. \quad (16b)$$

Our final equation can now be written in the following form:

$$\frac{\partial \bar{S}}{\partial t} + \frac{1}{A} \int_{\partial D} \bar{v}_j n_j \bar{S} dl = \frac{1}{A} \int_{\partial D} D_{ij}(\mathbf{x}, t) n_i \nabla_j \bar{S}(t, \mathbf{x}) dl. \quad (17a)$$

The dispersion coefficient  $D_{ij}(\mathbf{x}, t)$  is computed at the midpoint of the edge by

$$D_{ij}(\mathbf{x}, t) = \frac{1}{h_E} \int_{\partial E} \left[ \int_0^t v'_i(\mathbf{x}) v'_j(\mathbf{x}(\tau)) d\tau \right] dl, \quad (17b)$$

where  $h_E$  is the length of the grid block edge.

Our system of coarse-scale equations is now fully defined. Specifically, we solve the coarse-scale pressure equation (2a) (with  $\mathbf{k}^*$  in place of  $\mathbf{k}$ ) to obtain the coarse-scale velocity  $\bar{\mathbf{v}}$  and then solve (17) for the coarse-scale saturation  $\bar{S}$ . Several additional issues remain to be addressed, however, before an

actual numerical scheme can be implemented. The two key issues are (1) how do we obtain the fluctuating components of velocity ( $\mathbf{v}'$ ) and (2) how can these  $\mathbf{v}'$  best be used in numerical computations. We now address these two issues.

As discussed above, we would ultimately like to avoid the solution of a global fine-scale pressure equation to obtain the  $\mathbf{v}'$ . However, in the results presented below, we do, in fact, solve the global fine-scale problem to obtain the  $\mathbf{v}'$ . We proceed in this way because our intent in this paper is to demonstrate the applicability of the overall approach. Therefore, for present purposes, we prefer to avoid the additional approximations that would enter were we to estimate the  $\mathbf{v}'$  from the solution of local problems.

Several alternatives to the solution of the global fine-scale problem do exist, however, and some of these were explored. One approach is to estimate the  $\mathbf{v}'$  from the local fine-grid problems which are solved in the calculation of the grid block  $\mathbf{k}^*$ . We compared these  $\mathbf{v}'$  to those obtained from the global fine-grid solution of the pressure equation for a limited set of cases. We found very good correlation between these two sets of  $\mathbf{v}'$  (correlation coefficients of about 0.8–0.9) for the cases considered. This correlation improved slightly when we coarsened the fine grid nonuniformly (as described above) rather than uniformly. This suggests that the  $\mathbf{v}'$  computed from local solutions are sufficiently accurate to be used in our coarse-grid solutions. We did, in fact, use  $\mathbf{v}'$  computed from local fine-grid solutions of the pressure equation in a limited number of cases and saw only a slight degradation in accuracy.

Another alternative is to use a multiscale finite element method for the solution of the pressure equation [Hou and Wu, 1997; Efendiev, 1999]. The idea of this method is to capture the fine-grid information through the base functions constructed in each coarse-scale element (coarse block in our case). These base functions contain the fine-scale information which can then be used to compute the  $\mathbf{v}'$  in each coarse block. This approach represents a very natural means for incorporating subgrid information into coarse-scale calculations. However, because the results presented below were computed within a finite difference/finite volume context, we do not present any results using the multiscale finite element method.

We next address the actual computation of  $D_{ij}$ . The calculation of  $D_{ij}$  as a full two-point correlation function (as indicated by (17b)) would be very time-consuming computationally. Further, it is not necessarily desirable to represent  $D_{ij}$  in this way. This is because, owing to boundary effects and the fact that we wish to consider permeability fields with large correlation lengths and variances, the two-point correlation function may exhibit large fluctuations on the coarse scale. This could significantly complicate numerical calculations. Therefore we shall proceed in a different manner and attempt to model the  $D_{ij}$  term semiempirically.

We first note that we can rewrite (17b) as follows:

$$\begin{aligned} D_{ij}(\mathbf{x}, t) &= \frac{1}{h_E} \int_{\partial E} \left[ v'_i(\mathbf{x}) \int_0^t v'_j(\mathbf{x}(\tau)) d\tau \right] dl \\ &= \frac{1}{h_E} \int_{\partial E} \left[ v'_i(\mathbf{x}) \int_0^t v'_j(\mathbf{x}(\tau)) d\tau \right] dl, \end{aligned} \quad (18)$$

where  $\mathbf{x}(\tau)$  is the coarse trajectory, such that  $\mathbf{x}(t) = \mathbf{x}$ . The dispersion coefficient written in this way can be seen to be proportional to the magnitude of the velocity fluctuations in

the coarse block and a length scale associated with the distance traveled along the streamline. Therefore, on the basis of the form of (18) and dimensional considerations, we suggest that the diagonal components of  $D_{ij}$  can be modeled in the following form:

$$D_{ii}(\mathbf{x}, t) \approx \alpha(\sigma, l_x, l_z) L_i(\mathbf{x}, t) |v'_i(\mathbf{x})|, \quad (19)$$

where  $L_i$  is the length of the coarse-grid streamline in the  $i$  direction,  $|v'_i|$  is the magnitude of the  $i$  component of the velocity fluctuation, and  $\alpha(\sigma, l_x, l_z)$  is an empirical function, with  $\sigma^2$  being the variance and  $l_x$  and  $l_z$  being the correlation lengths of the permeability field. Note that in (19) there is no sum on repeated indices.

Numerical simulations indicated that  $\alpha$  is a strong function of  $\sigma$  but only a weak function of  $l_x$  and  $l_z$  for the moderate to large values of  $l_x$  we wish to consider. On the basis of a limited set of runs we estimated the following form for  $\alpha$ :

$$\alpha = (\sigma/2)^4. \quad (20)$$

We did not attempt to account for the weak dependence of  $\alpha$  on  $l_x$  and  $l_z$ , though our results could be improved slightly if we did account for these dependencies. We note that  $\alpha$  as defined in (20) is consistent with the result for  $D_{xx}$  in an infinite layered system, where  $x$  is the direction along the layering. Because we are interested in systems for which  $l_x \gg l_z$ , layered systems may be appropriate models for our case. For the layered case it can be shown that, for small  $\sigma$ ,  $\alpha \approx a \exp(2\sigma^2)$ , where  $a$  is a constant. This corresponds to an  $\alpha(\sigma)$  that is numerically quite close to the result given in (20) over the range of interest in  $\sigma$ ,  $1 \leq \sigma \leq 2$  (this agreement may, however, be simply fortuitous because these values of  $\sigma$  are not technically small). In any event, there is at least some consistency between our approximation of  $D_{ii}$  and  $\alpha$  and analytical results for layered systems.

This concludes our description of the governing equations. We now describe the numerical implementation of the overall procedure.

#### 4. Numerical Considerations

We now briefly consider some of the numerical issues that arise in our calculations. For the fine- and coarse-grid problems we solve the pressure equation using a standard finite difference approach, with transmissibilities computed using harmonic averages of the appropriate permeability component ( $\mathbf{k}$  and  $\mathbf{k}^*$  are taken to be diagonal). The nonuniformly coarsened grid for the coarse-scale problems is established through application of previously developed procedures; for details on this methodology see *Durlofsky et al.* [1996, 1997]. Basically, the method acts to introduce finer gridding in high-flow regions and coarser gridding elsewhere. This improves the quality of the model compared to a uniformly coarsened system though, as discussed in section 2, the method by itself is suitable for only moderate degrees of coarsening and cannot provide accurate results for highly coarsened systems. For the results presented below in which we introduce our subgrid dispersivity, the nonuniform gridding does not appear to be essential; comparable results were obtained in many cases with uniform grids. This is because the additional unresolved effects introduced by uniform coarsening are accurately represented with the subgrid dispersivity model. However, as indicated in section 3, nonuniform coarsening does act to improve the

accuracy of the subgrid  $\mathbf{v}'$  computed locally relative to those computed globally.

We solve the saturation equation for the fine-grid model and the nonuniformly coarsened model (with no dispersivity) by integrating along streamlines. This is a very accurate method and is essentially free of numerical dispersion. This approach cannot, however, be applied to the solution of the saturation equation with the subgrid dispersivity term. Rather, in this case we apply a finite volume scheme. In order to reduce numerical diffusion, we use a second-order total variation diminishing scheme for the convective terms in the solution [Sweby, 1984; Chen et al., 1993]. Integration in time is first-order, though we take small time steps to further reduce numerical dispersion. Although the overall solution method is second-order accurate in space, the method will lose accuracy as the grid becomes very coarse. Therefore we do not consider models much coarser than  $10 \times 10$  (regardless of the dimensions of the fine grid).

The dispersion term is computed from subgrid velocity fluctuations, as described in section 3. We update this term in space and time by integrating back along streamlines (on the coarse-grid model). This is a computationally efficient procedure because, at each time step, the additional contribution to  $D_{ij}$  involves only a few calculations. Once the dispersivity is computed at each grid block face, the dispersive fluxes through each face can be readily computed.

Because the dispersion term increases the order of the equation, we require additional boundary conditions. On no-flow boundaries the normal dispersive flux is zero because the fluctuations of the velocity in the normal direction are zero. Thus we do not need to impose any extra boundary conditions along no-flow boundaries. At the injection well we also do not need to impose any extra boundary conditions since the normal diffusive flux here is also zero. As we have only convective flux entering the system, we prescribe that there is only convective flux at the production well. This is equivalent to assuming that the normal dispersive flux is zero at the production well.

#### 5. Numerical Results

We now present a series of numerical results that demonstrate the accuracy and limitations of our proposed method. The systems we consider are intended to represent cross sections (in  $x - z$ ) of the subsurface; for that reason we take the system length in  $x$  ( $L_x$ ) to be 5 times the length in  $z$  ( $L_z$ ). All of the fine-grid permeability fields used in this study are  $100 \times 100$  realizations of prescribed overall variance ( $\sigma^2$ ) and correlation structure. The fields were generated using the Geostatistical Software Library (GSLIB) algorithms [*Deutsch and Journel*, 1998] with an exponential covariance model. In the examples below, we specify the dimensionless correlation lengths  $l_x$  and  $l_z$ , where each correlation length is nondimensionalized by the system length in the corresponding direction. For example,  $l_x = 0.3$  means that the actual correlation length of the permeability field is  $0.3L_x$ .

Because we model dispersivity as preasymptotic, our model is most applicable for the case of moderate to large  $l_x$ . The model would be expected to lose accuracy for very small correlation lengths, for which  $D_{ij}$  quickly reaches an asymptotic value. In the examples below, (except for the last case), we specify  $0.1 \leq l_x \leq 0.3$ . These values of  $l_x$  are not small and would not be expected to yield a constant dispersivity. Rather,

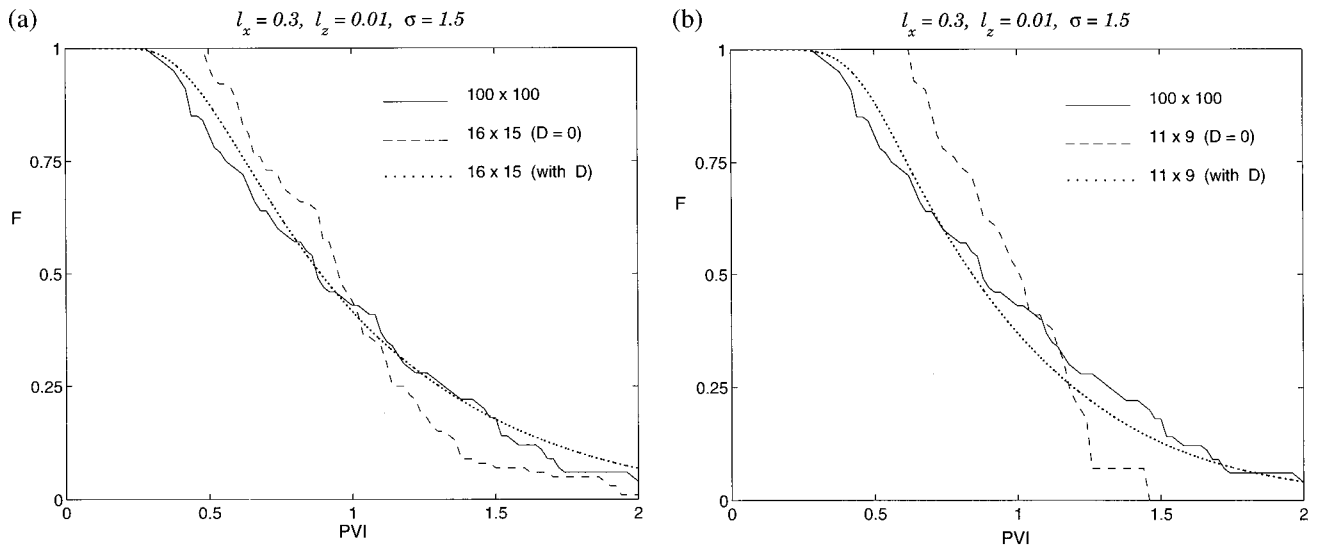


**Figure 1.** Fractional flow of displaced fluid at the production edge for the case  $l_x = 0.3$ ,  $l_z = 0.01$ , and  $\sigma = 1.5$ . Fine model is  $100 \times 100$ . In (a) coarse models are  $16 \times 15$ ; in (b) coarse models are  $11 \times 9$ . In Figures 1a and 1b and all subsequent figures the solid curves designate the fine-grid solution, the dashed curves designate the coarse-grid solution with no subgrid model, and the dotted curve designates the coarse-grid solution using our subgrid model for  $D_{ij}$ . Note the clear improvement in coarse scale results when the subgrid model is introduced.

the dispersivity would be expected to be preasymptotic, at least over much of the domain, suggesting our model should apply.

In all of the calculations below, we specify a fixed pressure and a constant saturation ( $S = 1$ ) at the inlet edge of the model ( $x = 0$ ) and a fixed pressure at the outlet edge ( $x = L_x$ ) of the model. The top and bottom boundaries are closed to flow. Results are presented in terms of fractional flow of displaced fluid ( $F$ , defined as the ratio of displaced fluid to total fluid produced) at the outlet edge versus pore volumes injected (PVI). PVI is analogous to dimensionless time and is defined as  $qt/V_p$ , where  $q$  is the total volumetric flow rate,  $t$  is dimensional time, and  $V_p$  is the total pore volume of the system.

Our first example (Figure 1a) is for the case  $l_x = 0.3$ ,  $l_z = 0.01$ , and  $\sigma = 1.5$ . In this and all subsequent figures the  $100 \times 100$  fine grid results are indicated by the solid line, the coarse-grid results using nonuniform coarsening only ( $D_{ij} = 0$ ) are indicated by the dashed line, and the coarse-grid results using our subgrid model for dispersivity are indicated by the dotted line. In this case the coarse models are of dimension  $16 \times 15$  (in the nonuniform coarsening procedure we do not specify the exact dimensions of the coarse model, so these dimensions are typically not “round” numbers). The nonuniformly coarsened results (with no dispersivity) overpredict breakthrough time and continue to overpredict the production of displaced fluid until  $t \sim 1.0$  PVI. This is consistent with the results of previous studies, which found that beyond a certain level of coarsening (approximately  $30 \times 30$  for this type of problem), nonuniform coarsening alone can no longer provide accurate coarse-scale results. It is evident from Figure 1a, however, that the introduction of our subgrid model noticeably improves the coarse-scale results. Specifically, the breakthrough of injected fluid (occurring at  $t \sim 0.27$  PVI) is now captured much more accurately, as is the general shape of the fractional flow curve.

The same behaviors are evident in Figure 1b, where we consider the same fine-grid realization but introduce higher

levels of upscaling in the coarse model (the coarse model in this case is  $11 \times 9$ ). Though the coarse model with dispersivity is not as accurate relative to the fine-grid model as in the previous case, we do observe a considerable improvement over the coarse-grid model with nonuniform coarsening only. This demonstrates that the subgrid dispersivity model correctly captures effects in the fine-grid permeability field that are unresolved in the nonuniformly coarsened model.

We next consider a case with a smaller correlation length in the  $x$  direction; here  $l_x = 0.2$ ,  $l_z = 0.01$ , and  $\sigma = 1.5$ . In Figures 2a and 2b we compare coarse-scale results of dimensions  $15 \times 15$  and  $11 \times 10$ , respectively, to the reference fine-grid results. The results with dispersivity are quite similar in the two cases and again demonstrate clear improvement over results using nonuniform coarsening only. Similar results are observed in Figures 3a and 3b for a different correlation structure ( $l_x = 0.1$ ,  $l_z = 0.025$ , and  $\sigma = 1.5$ ). In all calculations with  $\sigma = 1.5$  (Figures 1–3), the coarse grid results with the subgrid dispersivity model are more accurate in terms of breakthrough and overall curve shape than the results using nonuniform coarsening only.

The next set of results (Figures 4a and 4b) is for  $l_x = 0.2$ ,  $l_z = 0.01$  but with a higher variance,  $\sigma = 2$ . Though the coarse-scale results with dispersivity are clearly more accurate than the coarse-scale results using nonuniform coarsening only, they are not as accurate as the results presented above for the cases with  $\sigma = 1.5$ . This is especially evident in the  $11 \times 10$  coarse model (Figure 4b) at late times, that is, for  $t > \sim 0.7$  PVI. This may be due to the inaccurate estimation of dispersivity in the slower regions of the model.

The model displays better accuracy for the next case;  $l_x = 0.1$ ,  $l_z = 0.025$ , and  $\sigma = 2$  (Figures 5a and 5b). Here the  $15 \times 13$  coarse-scale results with dispersivity are extremely accurate and the  $10 \times 9$  results continue to display reasonable accuracy. However, the same trend observed above is also apparent here, namely, an underprediction of fractional flow at late times.

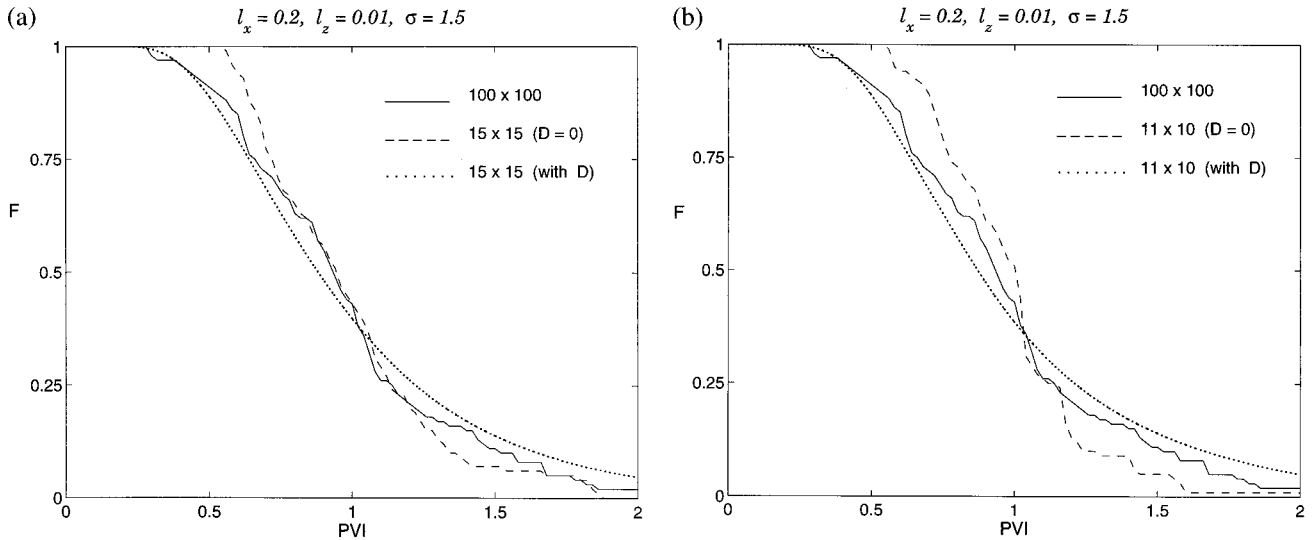


**Figure 2.** Fractional flow of displaced fluid at the production edge for the case  $l_x = 0.2$ ,  $l_z = 0.01$ ,  $\sigma = 1.5$ . Fine model is  $100 \times 100$ . Coarse models are (a)  $15 \times 15$  and (b)  $11 \times 10$ .

The next case considered is of lower variance:  $l_x = 0.2$ ,  $l_z = 0.01$ , and  $\sigma = 1$ . The coarse-scale results using the subgrid model on a grid of dimensions  $13 \times 13$  (Figure 6a) are very accurate. In this case the results using nonuniform coarsening only are also reasonably accurate, though the model with dispersivity provides a clear improvement. Results for a very coarse model ( $8 \times 7$ ) are shown in Figure 6b. Our subgrid treatment continues to provide results in close agreement with the reference fine-scale results for this case.

From the results presented in Figures 1–6, the subgrid dispersivity model is seen to provide considerably more accurate predictions than those obtained using only nonuniform coarsening for the systems considered. However, because the model represents dispersivity as continually evolving (i.e., preasymptotic), it would not be expected to be appropriate for systems with very small correlation lengths. To demonstrate the inaccuracy of the method for this case, we consider a permeability field with correlation structure  $l_x = 0.04$ ,  $l_z = 0.01$ , and  $\sigma =$

1.5. Flow results for this system for the fine-grid model and for coarse-grid models of dimensions  $16 \times 15$  are shown in Figure 7. As expected, our subgrid model significantly overestimates dispersivity and as a result predicts an earlier breakthrough time and lower production at early time than the fine-grid model.

Because the correlation length is quite small for this problem (approximately 1.5 correlation lengths in  $x$  per coarse-grid block), we would expect that better accuracy in the coarse-grid model could be obtained through use of a constant diffusivity rather than a continually evolving dispersivity. This is indeed the case, as demonstrated by the dotted-dashed curve in Figure 7. This curve was generated using a constant value of diffusivity ( $D_{xx}$ ) of 0.02. This value was obtained through trial and error and provides the best fit to the fine-grid results. In total, the results in Figure 7 demonstrate that at dimensionless correlation lengths less than some minimum, our subgrid dispersivity model loses accuracy and a conventional constant diffusivity

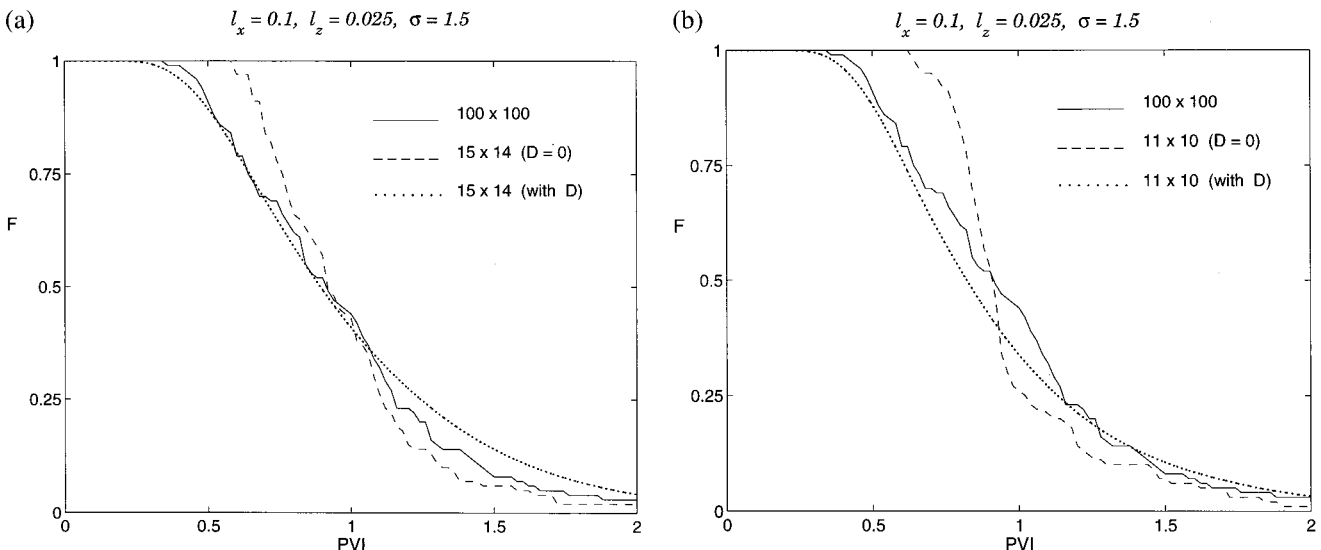


**Figure 3.** Fractional flow of displaced fluid at the production edge for the case  $l_x = 0.1$ ,  $l_z = 0.025$ ,  $\sigma = 1.5$ . Fine model is  $100 \times 100$ . Coarse models are (a)  $15 \times 14$  and (b)  $11 \times 10$ .

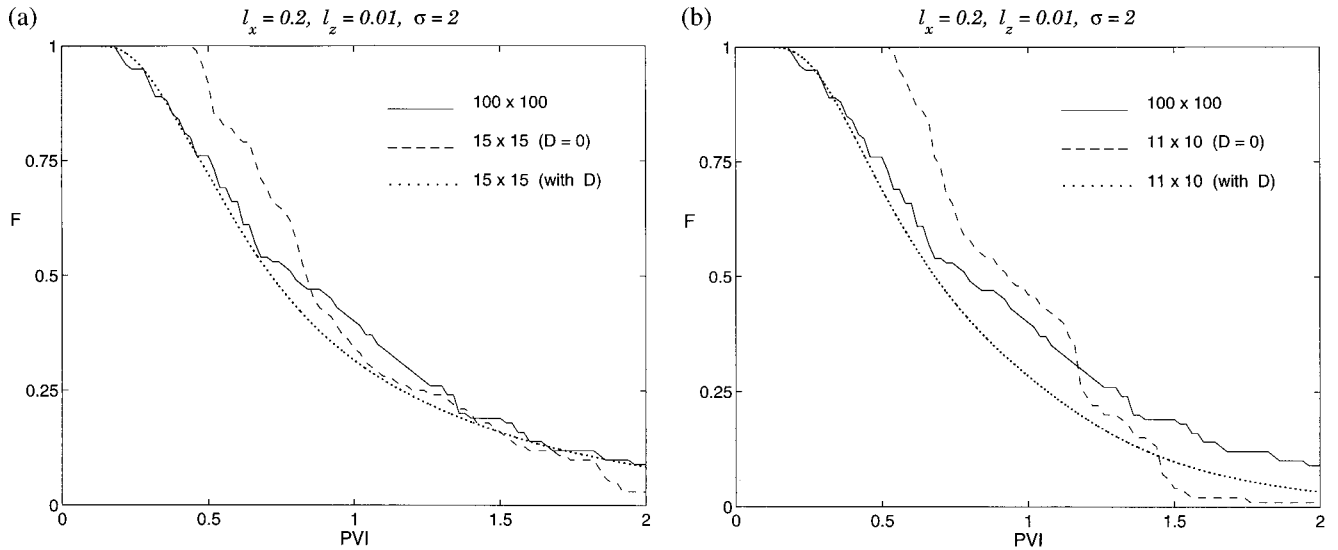


**Figure 4.** Fractional flow of displaced fluid at the production edge for the case  $l_x = 0.2$ ,  $l_z = 0.01$ , and  $\sigma = 2$ . Fine model is  $100 \times 100$ . Coarse models are (a)  $15 \times 15$  and (b)  $11 \times 10$ .

model is more appropriate. This suggests that the subgrid model could be further refined through the introduction of an upper cutoff for dispersivity, representing the asymptotic value. This type of treatment was not necessary for the cases considered in Figures 1–6 because the assumption of a continuously evolving dispersivity is valid for those systems. However, for more general cases such a treatment may prove useful.

## 6. Discussion and Conclusions

In this paper, we presented a procedure for incorporating subgrid effects, in the form of a position- and time-dependent dispersivity, into coarse-grid models of flow through heterogeneous formations. Through extensive numerical examples the subgrid treatment was shown to provide a considerable improvement in accuracy over that observed in simulations without the subgrid model. The overall procedure entails the non-

uniform coarsening of the fine-grid model (in a manner that retains dominant high-flow regions), the calculation of equivalent grid block permeability tensors, and the subsequent solution of the coarse-grid pressure equation. The subgrid velocity fluctuations are estimated from the solution of the fine-grid pressure equation, which allows for the calculation of a position- and time-dependent dispersivity. This dispersivity is then used in the coarse-scale solution of the saturation equation.

The approach presented here is strictly applicable only for unit mobility ratio displacements. In such problems the pressure and velocity fields do not change during the course of the simulation. In the more general case of immiscible displacement (nonunit mobility ratio), the pressure and velocity fields evolve during the course of the simulation (through the  $\lambda(S)$  term in (2a)) and must be updated. *Efendiev* [1999] considered the application of the methodology presented here to immis-

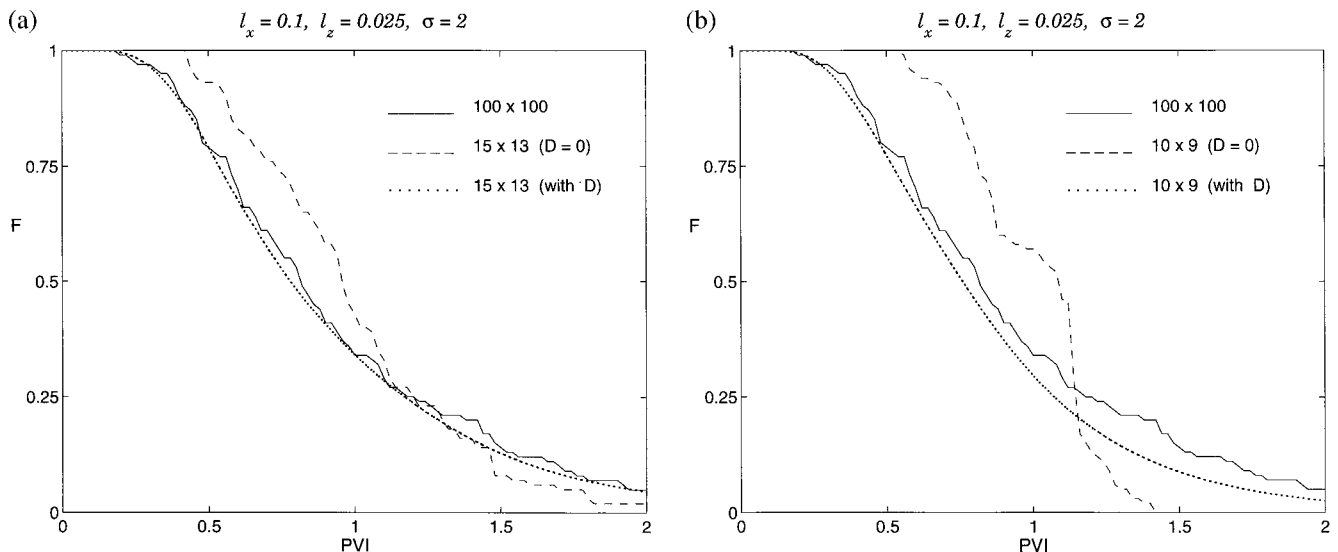


**Figure 5.** Fractional flow of displaced fluid at the production edge for the case  $l_x = 0.1$ ,  $l_z = 0.025$ , and  $\sigma = 2$ . Fine model is  $100 \times 100$ . Coarse models are (a)  $15 \times 13$  and (b)  $10 \times 9$ .

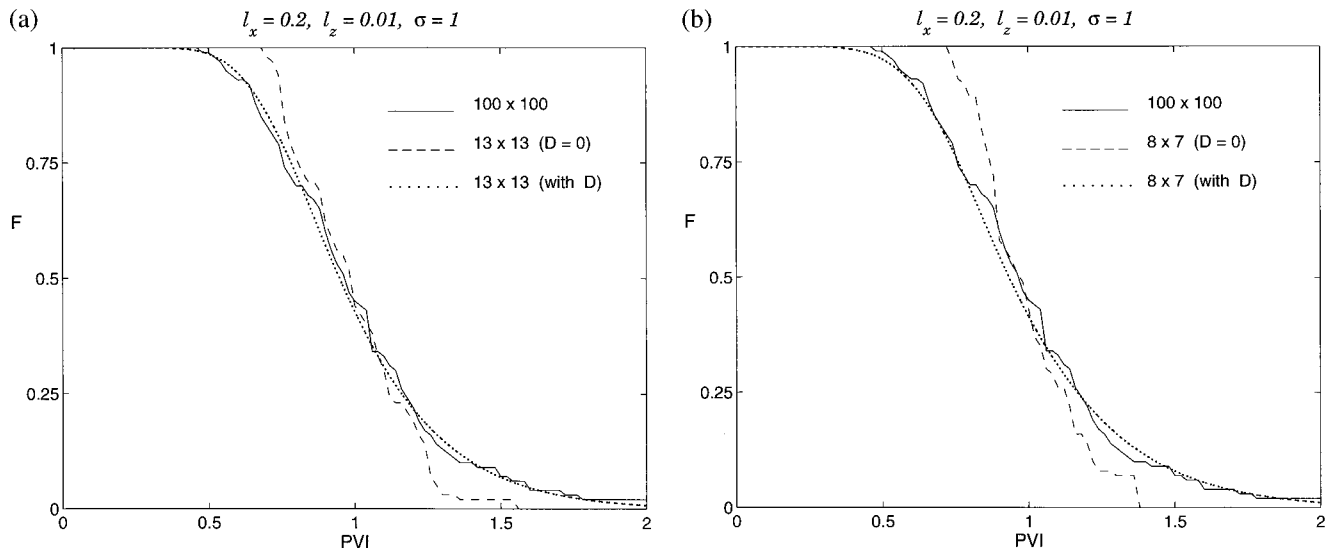


**Figure 6.** Fractional flow of displaced fluid at the production edge for the case  $l_x = 0.2$ ,  $l_z = 0.01$ , and  $\sigma = 1$ . Fine model is  $100 \times 100$ . Coarse models are (a)  $13 \times 13$  and (b)  $8 \times 7$ .

cible displacements. He showed that the basic approach can be applied to the more general case under the approximation that the streamlines do not change during the course of the simulation. This is a reasonable approximation in many cases; although the flow rates along streamlines may change considerably over the simulation, the streamlines themselves may change relatively slightly. The numerical results of Efendiev, for the nonunit mobility ratio case with fixed streamlines and no updating of the velocity field, are of comparable accuracy to the results presented in section 5. However, the method still requires further extension and evaluation before it is applicable to the modeling of general immiscible displacements.

The method could also be generalized in other areas as well. The current dispersivity model contains some semiempirical

elements that would presumably benefit from a firmer theoretical basis. Also, the method as currently implemented is strictly applicable only for the preasymptotic period. To be fully general, the method must recognize when  $D_{ij}$  has reached its asymptotic value and should no longer be updated. This will also provide for improved accuracy in more general situations, for example, when flow is skew to the direction of high correlation length. Existing asymptotic results, or results computed using the method of Rubin *et al.* [1999], might be useful in generalizing the model in this regard. Finally, the use of purely local fine-grid information for the estimation of  $\mathbf{v}'$  (or the use of a single fine-grid calculation in the case of nonunit mobility ratio) will be required for the method to attain maximum efficiency. In future work we plan to address these important technical issues.

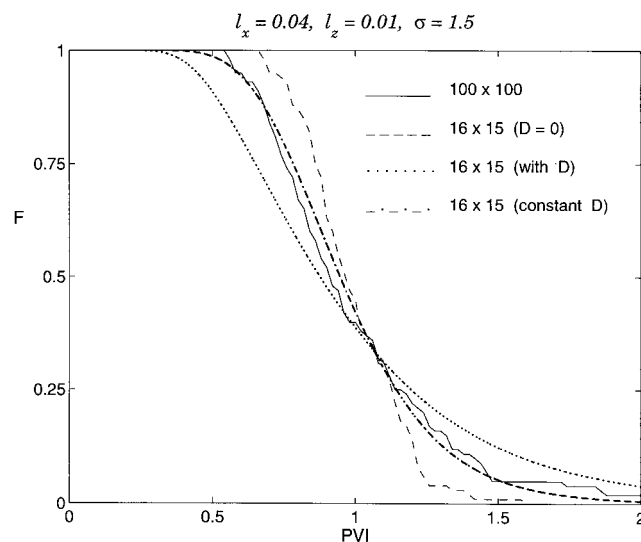


**Figure 7.** Fractional flow of displaced fluid at the production edge for the case  $l_x = 0.04$ ,  $l_z = 0.01$ ,  $\sigma = 1.5$ . Fine model is  $100 \times 100$ ; coarse models are  $16 \times 15$ . The dotted-dashed curve represents the coarse grid result using a constant, optimal diffusivity. Note that our subgrid model (dotted curve) significantly overestimates dispersivity in this case.

**Acknowledgments.** We are grateful to Fabien Cherblanc (Stanford University) for several useful discussions and to Roger Beckie (University of British Columbia) for his insightful comments on an earlier version of this paper.

## References

- Barker, J. W., and S. Thibeau, A critical review of the use of pseudo-relative permeabilities for upscaling, *SPE Reservoir Eng.*, 12, 138–143, 1997.
- Beckie, R., A. A. Aldama, and E. F. Wood, The universal structure of the groundwater flow equations, *Water Resour. Res.*, 30, 1407–1419, 1994.
- Beckie, R., A. A. Aldama, and E. F. Wood, Modeling the large-scale dynamics of saturated groundwater flow using spatial filtering theory. 1, Theoretical development, *Water Resour. Res.*, 32, 1269–1280, 1996.
- Chen, W. H., L. J. Durlofsky, B. Engquist, and S. Osher, Minimization of grid orientation effects through use of higher-order finite difference methods, *SPE Adv. Technol. Ser.*, 1, 43–52, 1993.
- Christie, M. A., Upscaling for reservoir simulation, *JPT J. Pet. Technol.*, 48, 1004–1010, 1996.
- Dagan, G., Solute transport in heterogeneous porous formations, *J. Fluid Mech.*, 145, 151–177, 1984.
- Dagan, G., Theory of solute transport by groundwater, *Annu. Rev. Fluid Mech.*, 19, 183–215, 1987.
- Deutsch C., and A. G. Journel, *GSLIB: Geostatistical Software Library*

- and *User's Guide*, 2nd ed., 368 pp., Oxford Univ. Press, New York, 1998.
- Durlofsky, L. J., Numerical calculation of equivalent grid block permeability tensors for heterogeneous porous media, *Water Resour. Res.*, 27, 699–708, 1991.
- Durlofsky, L. J., Use of higher moments for the description of upscaled, process independent relative permeabilities, *SPE J*, 2, 474–484, 1997.
- Durlofsky, L. J., Coarse scale models of two phase flow in heterogeneous reservoirs: Volume averaged equations and their relationship to existing upscaling techniques, *Comput. Geosci.*, 2, 73–92, 1998.
- Durlofsky, L. J., R. A. Behrens, R. C. Jones, and A. Bernath, Scale up of heterogeneous three dimensional reservoir descriptions, *SPE J*, 1, 313–326, 1996.
- Durlofsky, L. J., R. C. Jones, and W. J. Milliken, A nonuniform coarsening approach for the scale up of displacement processes in heterogeneous porous media, *Adv. Water Res.*, 20, 335–347, 1997.
- Efendiev, Y., The multiscale finite element method and its applications, Ph.D. thesis, Calif. Inst. of Technol., Pasadena, 1999.
- Gelhar, L., *Stochastic Subsurface Hydrology*, 390 pp., Prentice-Hall, Englewood Cliffs, N. J., 1993.
- Graham, W., and D. McLaughlin, Stochastic analysis of nonstationary subsurface solute transport, 1, Unconditional moments, *Water Resour. Res.*, 25, 215–232, 1989.
- Hewett, T. A., and R. A. Behrens, Conditional simulation of reservoir heterogeneity with fractals, *SPE Form. Eval.*, 5, 217–225, 1990.
- Hou, T., and X. Wu, A multiscale finite element method for elliptic problems in composite materials and porous media, *J. Comput. Phys.*, 134, 169–189, 1997.
- Kitanidis, P. K., Prediction by the method of moments of transport in a heterogeneous formation, *J. Hydrol.*, 102, 453–473, 1988.
- Langlo, P., and M. S. Espedal, Macrodispersion for two-phase, immiscible flow in porous media, *Adv. Water Res.*, 17, 297–316, 1994.
- Neuman, S. P., Eulerian-Lagrangian theory of transport in space-time nonstationary velocity fields: Exact nonlocal formalism by conditional moments and weak approximation, *Water Resour. Res.*, 29, 633–645, 1993.
- Renard, P., and G. de Marsily, Calculating equivalent permeability: A review, *Adv. Water Res.*, 20, 253–278, 1997.
- Rubin, Y., Stochastic modeling of macrodispersion in heterogeneous porous media, *Water Resour. Res.*, 26, 133–141, 1990.
- Rubin, Y., A. Sun, R. Maxwell, and A. Bellin, The concept of block-effective macrodispersivity and a unified approach for grid-scale and plume-scale-dependent transport, *J. Fluid Mech.*, 395, 161–180, 1999.
- Sweby, P. K., High resolution schemes using flux limiters for hyperbolic conservation laws, *SIAM J. Numer. Anal.*, 21, 995–1011, 1984.
- Wallstrom, T. C., S. Hou, M. A. Christie, L. J. Durlofsky, D. H. Sharp, and Q. Zou, Effective medium boundary conditions for upscaling relative permeabilities, Upscaling Downunder Conference Proceedings, Commonw. Sci. and Indust. Res. Organ. Pet., Melbourne, Australia, Feb. 7–10, 2000.
- Wen, X.-H., and J. J. Gomez-Hernandez, Upscaling hydraulic conductivities in heterogeneous media: An overview, *J. Hydrol.*, 183, ix–xxxii, 1996.
- Zhang, D., L. Li, and H. A. Tchelepi, Stochastic formulation for uncertainty assessment of two-phase flow in heterogeneous reservoirs, paper presented at the SPE Reservoir Simulation Symposium, Soc. of Pet. Eng., Houston, Tex., Feb. 14–17, 1999.
- Zhang, Q., The asymptotic scaling behavior of mixing induced by a random velocity, *Adv. Appl. Math.*, 16, 23–58, 1995.

---

L. J. Durlofsky, Department of Petroleum Engineering, Stanford University, Green Earth Sciences Building, Room 065, Stanford, CA 94305-2220. (lou@pangea.stanford.edu)

Y. Efendiev, Institute for Mathematics and Its Applications, University of Minnesota, 400 Lind Hall, 207 Church Street SE, Minneapolis, MN 55455. (efendiev@ima.umn.edu)

S. H. Lee, Chevron Petroleum Technology Company, P.O. Box 6019, San Ramon, CA 94583-0719. (seon@chevron.com)

(Received October 25, 1999; revised May 1, 2000; accepted May 2, 2000.)

